Conductivity and paraconductivity in $(Bi,Pb)_2Sr_2Ca_{n-1}Cu_nO_x$ whiskers

X-F Chen, M. J. Marone, G. X. Tessema, M. J. Skove, and M. V. Nevitt
Department of Physics and Astronomy, Clemson University, Clemson, South Carolina 29634

D. J. Miller and B. W. Veal
Argonne National Laboratory, Argonne, Illinois 60439
(Received 13 October 1992; revised manuscript received 21 January 1993)

We have measured the resistivity of $(Bi,Pb)_2Sr_2Ca_{n-1}Cu_nO_x$ single-crystal whiskers in the a and c directions. Our results indicate that the whiskers may be either 2:2:1:2 ($n=1$) or 2:2:2:3 ($n=2$) or have both phases present. Well above T_c, the resistivity in the a direction decreases linearly with temperature. We also studied the paraconductivity due to thermal fluctuations above T_c. The paraconductivity in the a direction shows quasi-one-dimensional behavior for temperatures close to T_c. This quasi-one-dimensional behavior may be due to a percolative conduction path. For the c direction, the resistivity is best fit by $\rho_c = Ae^{-E_g/kT}$, where T is the temperature. However, as T approaches T_c from above, ρ_c increases much faster than a thermally activated law, perhaps because of the fluctuations.

The properties of Bi-based high-T_c crystals are strongly anisotropic.[1] The reason for this anisotropy lies in the crystal structure: the high conductivity Cu-O planes (along the a-b plane) are separated by low conductivity layers (in the c direction). This anisotropy leads to differences in the temperature dependence of the resistivity for the a and c directions: metallic ($dR/dT>0$) in the a direction and nonmetallic ($dR/dT<0$) along the c axis.[2,3] The difference between the 2:2:0:1, 2:2:1:2, and 2:2:2:3 phases of $(Bi,Pb)_2Sr_2Ca_{n-1}Cu_nO_x$ ($n=1,2,3$) is in the number of layers of calcium and copper oxides. It is very hard to grow pure 2:2:2:3 single crystals that do not contain some 2:2:1:2 or 2:2:0:1 phases.[4,5] Our whisker samples have varying proportions of the 2:2:1:2 and 2:2:2:3 phases.

$(Bi,Pb)_2Sr_2Ca_{n-1}Cu_nO_x$ samples were grown by annealing a glass as specified by Matsubara *et al.*[6,7] The ratio of Pb to Bi was either 0 or 0.248. Starting powders were well mixed and melted at 1200 °C for 30 min. This molten material was then quenched to room temperature in about 2 s to form a glassy material. Whiskers were grown by annealing the resulting glassy material in an O_2 flow at 840 °C for 5 days and then cooling in O_2 to room temperature. Typical dimensions of the whiskerlike crystals were (0.5–7 mm)× (10–100 μm)×(1–10 μm).

Samples were characterized by electron diffraction, magnetization, and resistance R versus temperature T measurements. Selected area electron diffraction (SAD) was used with energy dispersive spectroscopy (EDS) analysis on a Philips 420 transmission electron microscope operated at 100 kV to identify the structure of some of the whiskers. Figure 1 shows the SAD patterns from one of the samples. The patterns can be indexed consistently with the 2:2:1:2 phase. Both the selected area and the convergent beam electron-diffraction patterns remain unchanged when the sample is translated beneath the beam suggesting a nearly single-crystalline whisker. The SAD patterns indicate that the c axis is normal to the long axis of the whisker. The b axis can be identified by the superlattice reflections and, based on the relative orientation between diffraction pattern and image, show that the whiskers grow with the long axis parallel to the a axis. EDS analysis shows that the atomic percentages of each element and the stoichiometry of the sample is within 95% of that of 2:2:1:2, consistent with the identification based on electron diffraction.

Magnetization measurements were made with a SQUID magnetometer. The results for a typical sample are shown in Fig. 2. The transition temperature for this sample is $T_c=81$ K. SQUID measurement on a 2:2:2:3 sample has also revealed a single transition at 107 K.

Contacts for resistance measurements were mounted using silver paint (Dupont No. 5007). For c-direction resistance measurements, the Montgomery method[8] has been widely used. This indirect way is not appropriate for our samples, since the smallest contact area we can make is not small compared to the size of our samples.[9] Since the resistance is highly anisotropic,[10] we used a simple four-contact method to measure the resistance along the a and c axes. The contact arrangement is shown in the inset of Fig. 3. In order to form the bottom contacts (contact nos. 1, 2, 3, 4), the sample was laid on four copper wires onto which small drops of silver paint had been placed. $NbSe_3$ whiskers were used for the four top contacts (contact nos. 5, 6, 7, 8). We made the droplets of silver paint as large as we could to promote uniform current flow, but small enough to avoid having the silver paint flow over an edge and short the c-axis resistance. For c-axis measurements, the current was passed through the two end wires on each side (contact nos. 1, 4, and 5, 8 shorted together). The voltage, $\Delta V=V_{2,3}-V_{6,7}$ was measured using the two middle wires, with contact nos. 2, 3 and 6, 7 shorted together on each side. Thus, the current was forced to be nearly uniform through the sample. For the a-direction measurements, we used the contacts at the two ends of one large

face as current leads (contact nos. 5, 8 or 1, 4). Voltage leads were formed by the middle pair on the same large face (contact nos. 6, 7 or 2, 3).

Figure 3 shows a typical plot of R_a and R_c versus T for phase pure samples. For simplicity we have chosen a sample with a single resistive transition. Both the c- and a-direction resistances go to zero at $T_c = 106$ K. The slope dR_c/dT is negative, while dR_a/dT is positive down to $T = T_c$. Similar results were obtained for 2:2:1:2 samples with a typical T_c of about 81 K. Mixed phase samples have been found which exhibit drops in the resistance R_a at two temperatures, corresponding to the 2:2:1:2 and 2:2:2:3 phases. In such samples, the drop in R_a at the critical temperature of the 2:2:2:3 phase is accompanied by an upward jump in R_c. However, the general features of the single-phase samples are still found in the mixed samples.

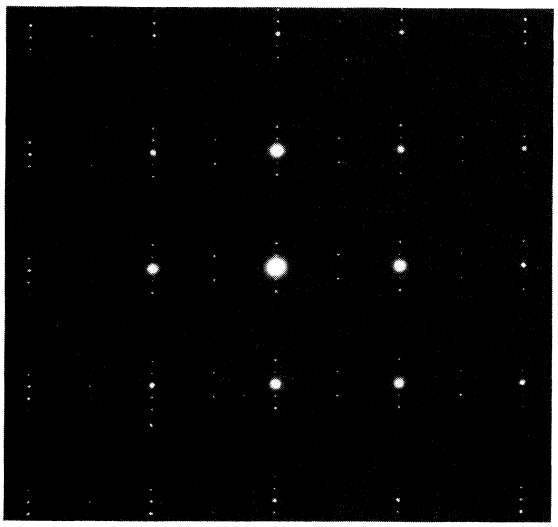

FIG. 1. Selected area diffraction (SAD) patterns from a (Bi, Pb)$_2$Sr$_2$Ca$_{n-1}$Cu$_n$O$_x$ whisker. The patterns are indexed according to the 2:2:1:2 phase.

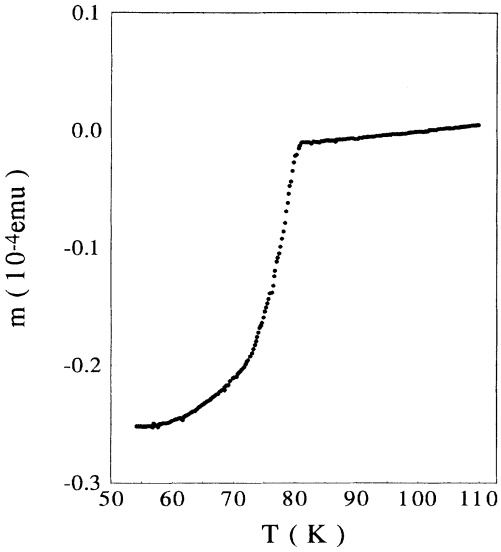

FIG. 2. Temperature dependence of the magnetization of a 2:2:1:2 sample.

Figure 4 shows a comparative plot of $\ln[R_c/R_{c0}]$ versus $1000/T$ and R_c versus $1000/T$, where R_{c0} is the room-temperature value of R_c. It is clear that the thermal activation law ($R \propto e^{-E_g/kT}$) gives a better fit to the c-axis resistance than does $R \propto 1/T$.[11] This is true between 120 K and room temperature for all 11 samples investigated. The average activation energy E_g can be estimated from this fit. For the 3 samples showing a transition corresponding to the 2:2:1:2 phase, E_g is (230±20) K or 20 meV. For the 8 samples showing a transition corresponding to the 2:2:2:3 phase, the average E_g is (250±20) K or 22 meV.

Near T_c, the a-axis resistance is no longer linear in T and the c-axis resistance deviates from the activated law

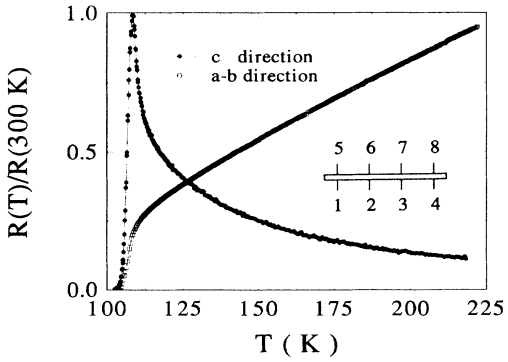

FIG. 3. Normalized resistance vs temperature curves for current flow parallel (R_a) and perpendicular (R_c) to the CuO layers of (Bi,Pb)$_2$Sr$_2$Ca$_{n-1}$Cu$_n$O$_x$. A sketch of the contact geometry is shown in the inset.

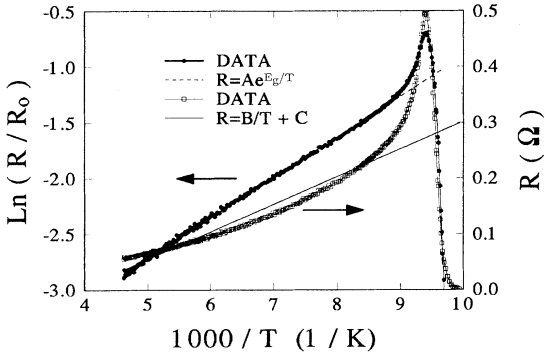

FIG. 4. Temperature dependence of the resistance along the c axis plotted as a function of $1000/T$. The activated law gives a better fit to the resistance data along the c axis.

$e^{-E_g/kT}$. We attribute these deviations to Aslamasov-Larkin fluctuations. The paraconductivity σ_p (above T_c) is defined to be the difference between the measured conductivity s_m and the extrapolated conductivity σ_e ($\sigma_p=\sigma_m-\sigma_e$). Above 210 K, the R versus T curve is very nearly linear and the extrapolated conductivity is obtained from this temperature range. In the mean-field region, the Aslamosov-Larkin (AL) theory[12,13] shows that the paraconductivity, in different dimensions, is given by

$$\sigma_p=\{e^2/[32\hbar\xi(0)]\}\tau^{-1/2}, \quad 3D\ , \tag{1a}$$

$$\sigma_p=[e^2/(16\hbar d)]\tau^{-1}, \quad 2D\ , \tag{1b}$$

$$\sigma_p=\{[e^2\xi(0)]/(16\hbar S)\}\tau^{-3/2}, \quad 1D\ , \tag{1c}$$

where $\tau=(T-T_c)/T_c$ is the reduced temperature, and d and S are the thickness and cross-sectional area of the sample, respectively. In high-T_c copper oxide superconductors, there exists an intrinsic two-dimensional (2D) Cu-O structure and large anisotropy between the c axis and the a-b plane. Because of this structure one would expect the paraconductivity to follow Eq. (1b). Results previously reported in the literature showed complicated properties of 3D,[14] 2D,[15,16] and crossover[17] of the dimensionality in high-T_c materials.

Assuming Aslamasov-Larkin behavior for the a-direction fluctuation, we find that the paraconductivity along the a axis σ_{p11} near the 2:2:2:3 transition temperature is proportional to $\tau^{-\lambda}$, where $\lambda=\frac{3}{2}$ as in Fig. 5. The mean λ obtained from eight samples is 1.52 ± 0.03. This implies that the fluctuations in these samples are 1D, perhaps because the conduction path is percolating through a 2:2:1:2 matrix. This is consistent with electron microscopy and magnetization measurements which show that the samples are at least 95% 2:2:1:2 phase. On the other hand, σ_{p11} for the three 2:2:1:2 samples investigated is also proportional to $\tau^{-\lambda}$ with $\lambda=(1.52\pm0.03)$.

It should be noted that measurements of σ_{p11} in larger single crystals of 2:2:1:2 yield values of λ between 0.33 and 1.[18] In films, where percolative conduction is probable, values of $\lambda=\frac{3}{2}$ have also been found.[19]

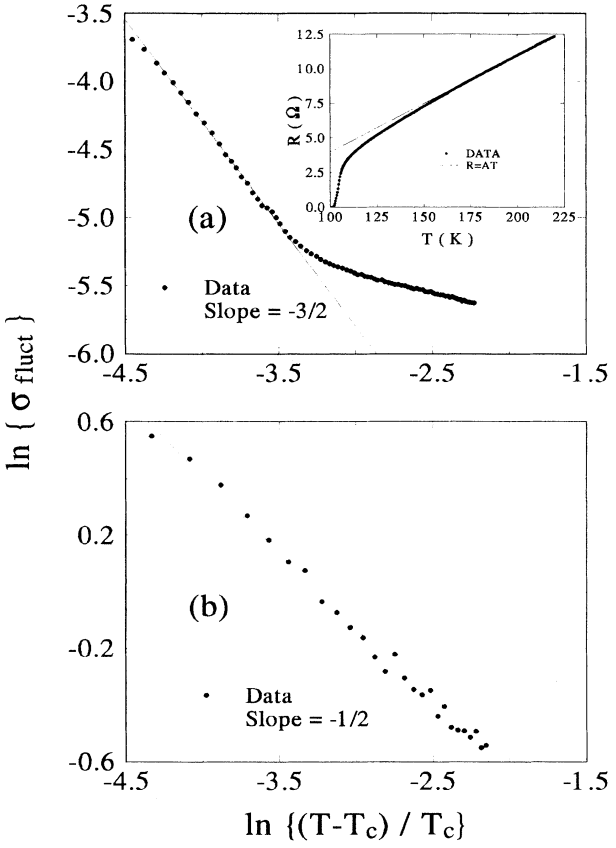

FIG. 5. (a) Paraconductivity in the a direction. The straight line shows a slope of $\frac{3}{2}$ expected for 1D. (b) Analysis of the "pararesistivity" along the c axis. The straight line is a fit using the 3D value for λ.

The temperature dependence of the conductivity in the c direction is also modified near T_c. We find an anomalous decrease in the c-axis conductivity above T_c. Using a similar approach as in the a-axis paraconductivity, we defined a so-called "pararesistivity" ρ_{pc} as the difference between the measured resistivity and the extrapolated resistivity. Analyzing this pararesistivity using the same formalism as σ_{p11}, we observe that $\sigma_{pc}=[\rho_{pc}]^{-1}$ is proportional to $\tau^{-1/2}$ [Fig. 5(b)]. This behavior has been reproduced on 11 samples giving a power $\lambda=\frac{1}{2}$. This suggests that if the enhanced resistivity near T_c were due to fluctuations they would be 3D "resistive" fluctuations. This unusual decrease in conductance may be due to the reduction in the number of normal carriers caused by the fluctuations in the a-b plane. It could also be due to an increase in the tunneling resistance across the CuO layers as they become superconducting.

Fitting Eqs. (1a)–(1c) to the experimental data is usually very sensitive to the choice of the value of T_c and to the extrapolated slope of the R versus T relation. The following equation[19]

$$d\sigma_p/dT\approx(\sigma_p)^{(1+\lambda)/\lambda} \tag{2}$$

allows an alternative determination of λ independent of the value of T_c. A log-log plot of $-d\sigma_p/dT$ versus σ_p will provide the value of λ, and therefore the dimensionality of the fluctuations. Values of λ obtained from Eq. (2) were the same as in the previous analysis, 1D for the a direction and 3D for the c direction.

The 1D behavior of the excess conductivity in the a-b plane instead of the expected 2D behavior[15,16] may mean that the cross section of the samples is less than the correlation length or that there is a percolative structure in our samples despite the clearly single-phase electron-diffraction pattern and the single resistive and magnetic superconducting transitions. The correlation length measured in the a-b plane is about 1 nm. Our samples are typically about 100 μm wide and 10 μm thick. Thus, it is very unlikely that the fluctuations are due to the dimensions of our whiskers.

In conclusion, we have measured the in-plane and out-of-plane resistance of $(Bi,Pb)_2Sr_2Ca_{n-1}Cu_nO_x$ samples, which were grown from a glass and were well characterized. Resistance measurements show that the samples can be single phase 2:2:2:3, mixed phase of 2:2:2:3 and 2:2:1:2, or single phase 2:2:1:2. The SQUID results show some 2:2:2:3 but mostly the 2:2:1:2 phase. EDS and electron diffraction show mostly the 2:2:1:2 phase. These results indicate that there is a percolating 2:2:2:3 phase path with the majority of the sample being the 2:2:1:2 phase, causing the conductive fluctuations in the a direction to follow Aslamosov-Larkin one-dimensional behavior. However, a percolating path is not a reasonable explanation for 1D-like behavior in the single-phase 2:2:1:2 samples. Thus, both explanations of the 1D behavior (sample size and percolation path) do not seem to fit our 2:2:1:2 samples. Above the transition temperature, the c-axis conductance was fit by a thermal activation law. An activation energy of (230±20) K for the 2:2:1:2 phase and (250±20) K for the 2:2:2:3 phase was found. In both 2:2:2:3 and 2:2:1:2 samples, the c-axis resistivity near T_c increases faster than the activated behavior. We attributed this "pararesistivity" to freezing out of normal carriers, due to the fluctuations in the a-b plane. We show, however, that this c-axis "pararesistivity" follows a power law with $\lambda \approx \frac{1}{2}$, as do 3D Aslamosov-Larkin fluctuations.

[1]D. M. Ginsberg, *Physical Properties of High Temperature Superconductors II* (World Scientific, Singapore, 1990), p. 164.
[2]L. Forro, V. Ilakovac, and B. Keszei, Phys. Rev. B **41**, 9551 (1990).
[3]S. Martin, A. T. Fiory, R. M. Fleming, L. F. Schneemeyer, and J. V. Waszczak, Phys. Rev. B **41**, 846 (1990).
[4]Q. R. Feng, H. Zhang, S. Feng, X. Zhu, K. Liu, and L. Xue, Solid State Commun. **78**, 609 (1991).
[5]A. Gama, E. Chavira, and R. Escudero, Phys. Rev. B **42**, 2161 (1990).
[6]I. Matsubara, H. Kageyama, H. Tanigawa, T. Ogura, H. Yamashita, and T. Kawai, Jpn. J. Appl. Phys. **28**, L1121 (1989).
[7]X. F. Chen, G. X. Tessema, and M. J. Skove, Physica C **181**, 340 (1991).
[8]H. C. Montgomery, J. Appl. Phys. **42**, 2971 (1971).
[9]M. Charalambous, J. Chaussy, and P. Lejay, Physica B **169**, 637 (1991).
[10]B. Batlogg, Physics Today, June **44** (1991).
[11]P. W. Anderson and Z. Zou, Phys. Rev. Lett. **60**, 132 (1988).
[12]L. G. Aslamazov and A. I. Larkin, Phys. Lett. **26A**, 238 (1968).
[13]W. J. Skocpol and M. Tinkham, Rep. Prog. Phys. **38**, 1409 (1975).
[14]P. P. Freitas, C. C. Tsuei, and T. S. Plaskett, Phys. Rev. B **36**, 833 (1987).
[15]M. Ausloos and Ch. Laurent, Phys. Rev. B **37**, 611 (1988); S. Ravi and V. Seshu Bai, Physica C **182**, 345 (1991).
[16]J. A. Veria, J. Maza, and F. Videl, Phys. Lett. A **131**, 310 (1988); D. H. Kim, A. M. Goldman, J. H. Kang, K. E. Gray, and R. T. Kampwirth, Phys. Rev. B **39**, 12 275 (1989).
[17]R. K. Nkum and W. R. Datars, Physica C **192**, 215 (1992); P. Mandal, A. Poddar, A. N. Das, and B. Ghosh, *ibid.* **169**, 43 (1990).
[18]J. R. Cooper, V. Ilakovac, and L. Forro (unpublished).
[19]Q. Y. Ying and H. S. Kwok, Phys. Rev. B **42**, 2242 (1990).

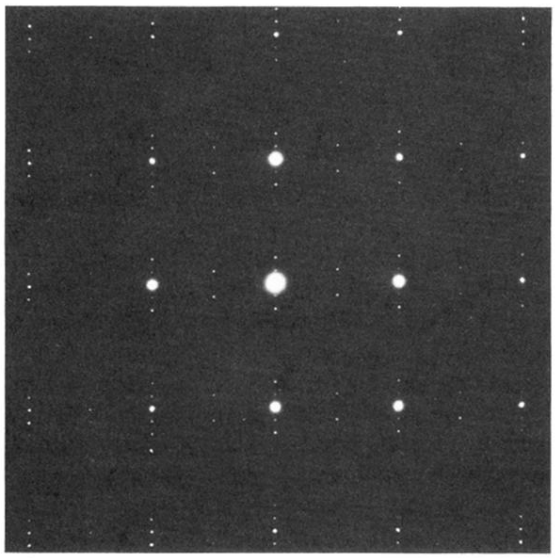

(a)

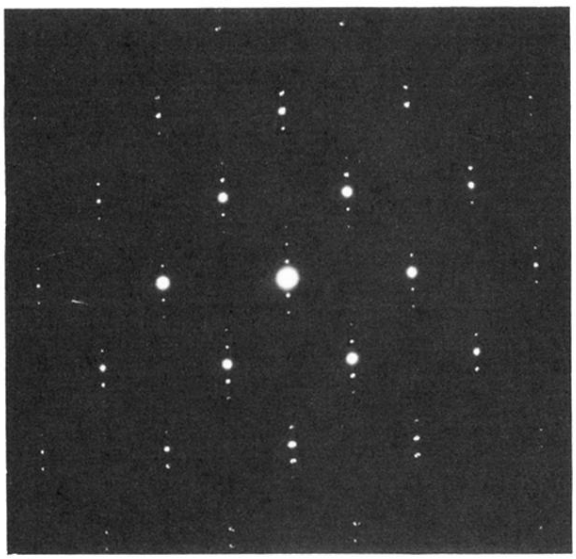

(b)

FIG. 1. Selected area diffraction (SAD) patterns from a $(Bi, Pb)_2Sr_2Ca_{n-1}Cu_nO_x$ whisker. The patterns are indexed according to the 2:2:1:2 phase.